HEPATOLOGY

HEPATOLOGY, VOL. 68, NO. 3, 2018

Landscape of Immune Microenvironment in Hepatocellular Carcinoma and Its Additional Impact on Histological and Molecular Classification

Yutaka Kurebayashi,[1] Hidenori Ojima,[1] Hanako Tsujikawa,[1] Naoto Kubota,[1] Junki Maehara,[1,3] Yuta Abe,[2] Minoru Kitago,[2] Masahiro Shinoda,[2] Yuko Kitagawa,[2] and Michiie Sakamoto[1]

Immune cells constitute an important element of tumor tissue. Accumulating evidence indicates their clinicopathological significance in predicting prognosis and therapeutic efficacy. Nonetheless, the combinations of immune cells forming the immune microenvironment and their association with histological findings remain largely unknown. Moreover, it is unclear which immune cells or immune microenvironments are the most prognostically significant. Here, we comprehensively analyzed the immune microenvironment and its intratumor heterogeneity in 919 regions of 158 hepatocellular carcinomas (HCCs), and the results were compared with the corresponding histological and prognostic data. Consequently, we classified the immune microenvironment of HCC into three distinct immunosubtypes: Immune-high, Immune-mid, and Immune-low. The Immune-high subtype was characterized by increased B-/plasma-cell and T cell infiltration, and the Immune-high subtype and B-cell infiltration were identified as independent positive prognostic factors. Varying degrees of intratumor heterogeneity of the immune microenvironment were observed, some of which reflected the multistep nature of HCC carcinogenesis. However, the predominant pattern of immunosubtype and immune cell infiltration of each tumor was prognostically important. Of note, the Immune-high subtype was associated with poorly differentiated HCC, cytokeratin 19 (CK19)$^+$, and/or Sal-like protein 4 (SALL4)$^+$ high-grade HCC, and Hoshida's S1/Boyault's G2 subclasses. Furthermore, patients with high-grade HCC of the predominant Immune-high subtype had significantly better prognosis. These results provide a rationale for evaluating the immune microenvironment in addition to the usual histological/molecular classification of HCC. *Conclusion*: The immune microenvironment of HCC can be classified into three immunosubtypes (Immune-high, Immune-mid, and Immune-low) with additional prognostic impact on histological and molecular classification of HCC. (HEPATOLOGY 2018; 68:1025-1041)

Immune cells constitute an important element of tumor tissue, and the amount of immune cell infiltration considerably differs among tumor types and histological subtypes.[1,2] The recent success of immune checkpoint inhibitors as potential treatments for hepatocellular carcinoma (HCC)[3] has raised interest in the evaluation of local and systemic antitumor immunity. In addition to CD8$^+$ T cells and natural killer (NK) cells that play pivotal roles in antitumor immunity, tumor tissue also contains various adaptive and innate immune cells, forming a complex immune microenvironment. Tumor progression is generally associated with the exclusion of these effector lymphocytes and the accumulation of regulatory T cells

Abbreviations: CK19, cytokeratin 19; CTL, cytotoxic T lymphocyte; CXCL, chemokine (C-X-C motif) ligand; DC, dendritic cell; EBI3, Epstein Barr virus-induced gene 3; EpCAM, epithelial cell adhesion molecule; GS, glutamine synthetase; HCC, hepatocellular carcinoma; IL, interleukin; NK, natural killer; NKT, natural killer T; PD-1, programmed death 1; PD-L1, programmed death ligand 1; pDC, plasmacytoid dendritic cell; SALL4, Sal-like protein 4; Th1, type 1 T helper; Treg, regulatory T cell.

Received October 13, 2017; accepted March 25, 2018.

Additional Supporting Information may be found at onlinelibrary.wiley.com/doi/10.1002/hep.29904/suppinfo.

Supported by a Grant-in-Aid for Research Activity start-up (JP17H07089 to Y.K.) and, in part, supported by a Grant-in-Aid for Scientific Research (B) (JP26293081 to M.S.) from the Japan Society for the Promotion of Science.

View this article online at wileyonlinelibrary.com.

DOI 10.1002/hep.29904

Potential conflict of interest: Nothing to report.

(Tregs) and tumor-associated macrophages, and tumors with a regulatory immune microenvironment often exhibit poor prognosis.[2]

Despite this accumulating evidence, the exact combination of immune cells forming the immune microenvironment, their intratumor heterogeneity, and their association with histological findings are largely unknown. It is still unclear which immune cell and immune microenvironment are the most prognostically significant. Although recent studies have comprehensively analyzed immune cells in tumor tissues through gene-expression–based and flow cytometric/CyTOF based analyses,[4,5] comparison of the results with histological features is difficult using these methods. Immune cell detection by multiplex immunohistochemistry (IHC)[6,7] or mass spectrometry–based tissue imaging[8] enables a more direct and intuitive analysis of the immune microenvironment with histological information; however, such studies are still scarce.

HCC is the second- and fifth-leading cause of cancer-related death worldwide and in Japan, respectively.[9] Studies have shown that increased infiltrations of T, NK, and natural killer T (NKT) cells in HCC are positive prognostic factors,[10-12] and increased infiltration of Tregs is a negative prognostic factor.[13,14] The prognostic roles of B-cell and plasma-cell infiltration are controversial.[15-17] The combination of immune cells forming the immune microenvironment and the extent of its intratumoral heterogeneity are also unclear in HCC. Furthermore, the prognostic significance of histopathological findings and molecular profiling is still unsatisfactory, and more accurate indicators are required. It is also intriguing that HCC is a well-accepted model of multistep carcinogenesis,[18] because its study should help elucidate changes in the immune microenvironment during the course of tumor development.

To address these issues, we conducted comprehensive analyses of immune cells through multiplex IHC in 919 regions of 158 HCCs resected from 141 patients. The results were compared with histopathological features, molecular classifications, and prognostic data. We also analyzed the local cytokine/chemokine milieu in distinct immune microenvironments to elucidate possible mechanisms for the formation of these microenvironments.

Patients and Methods

PATIENTS AND SAMPLES

One hundred fifty-eight HCCs of 141 patients who underwent surgical resection at Keio University Hospital (Tokyo, Japan) in the periods 2004-2010 and 2015-2017 were enrolled in this study. Primary HCCs surgically resected between 2004 and 2016 were enrolled in the prognostic analysis (138 HCCs of 124 patients), in which no patients underwent previous therapies. Among the 20 HCCs surgically resected in 2017, five HCCs were relapsed cases, among which one HCC underwent previous transarterial chemoembolization (26 months before resection) and four HCCs underwent previous radiofrequency ablation. No cases underwent neoadjuvant chemotherapy using multikinase inhibitors (e.g., sorafenib), immune-checkpoint inhibitors, or immunotherapy. Clinical data, including age, sex, and etiology, were obtained from medical records and are shown in Supporting Tables S1 and S2. The median follow-up period of 138 HCCs enrolled in prognostic analysis was 1,559 days (range, 65-4,124). The study was performed in accord with the Declaration of Helsinki and was approved by the ethics committees of Keio University School of Medicine.

MULTIPLEX IHC

Multiplex IHC was performed as described[6]; the antibodies used in this study are listed in Supporting

ARTICLE INFORMATION:

From the [1]Department of Pathology, Keio University School of Medicine, Tokyo, Japan; [2]Department of Surgery, Keio University School of Medicine, Tokyo, Japan; and [3]Department of Clinical Radiology, Graduate School of Medical Sciences, Kyushu University, Fukuoka, Japan.

ADDRESS CORRESPONDENCE AND REPRINT REQUESTS TO:

Michiie Sakamoto, M.D., Ph.D.
Department of Pathology, Keio University School of Medicine
35 Shinanomachi, Shinjuku-ku
Tokyo 160-0016, Japan
E-mail: msakamot@z5.keio.jp
Tel: +81-3-5363-3764

Table S3. Representative IHC results are shown in Supporting Figs. S1 and S2. Detailed analytical methods are described in the Supporting Methods.

EXTRACTION OF mRNA AND REAL-TIME PCR

Fresh tumor tissues were macroscopically sampled from multiple regions exhibiting different macroscopic features per each HCC. Total mRNA was extracted from frozen tissues using an RNeasy Mini Kit (Qiagen, Hilden, Germany), and cDNA was reverse-transcribed using a PrimeScript RT Reagent Kit (Takara-Bio, Shiga, Japan). Real-time PCR was performed using a CFX96 Real Time PCR System (Bio-Rad, Hercules, CA), a C1000 Thermal Cycler (Bio-Rad), and SYBR Premix Ex Taq II (Takara-Bio). Expression levels were analyzed by the comparative C_T method. The primers used in this study were designed in reference to GET Prime 2.0[19] and are listed in Supporting Table S4.

STATISTICAL ANALYSIS

Correlation matrices were computed using the Pearson correlation coefficient. Univariate and multivariate analyses were performed using the Cox proportional hazards model. Kaplan-Meier curves were analyzed using the log-rank test. Hierarchical clustering, k-means clustering, and heat map generation were performed using MultiExperimental Viewer (MeV) v4.9[20] (also see the Supporting Methods for details). *P* values between unpaired and paired variables were calculated using the Mann-Whitney U test and the Wilcoxon signed-rank test, respectively. $P < 0.05$, $P < 0.01$, and $P < 0.001$ are denoted by single, double, and triple asterisks, respectively.

Results

EVALUATION OF THE LEVEL OF IMMUNE CELL INFILTRATION USING MULTIPLEX IHC

To comprehensively analyze the immune microenvironment in HCC, we evaluated the infiltration of both adaptive and innate immune cells in 919 regions of 158 HCCs using multiplex IHC. Representative results of multiplex IHC are shown in Supporting Figs. S1 and S2.

Of the adaptive and innate immune cells analyzed in this study, macrophages were the most common immune cells. The next-most abundant immune cells were $CD4^+$ and $CD8^+$ T cells, and the amount of T-cell infiltration considerably varied among regions (Fig. 1A). Other immune cells constituted a relatively minor component; however, regions exhibiting high infiltration of B cells, plasma cells, NK cells, or neutrophils were also observed (Fig. 1A). Infiltration of most immune cell types were positively correlated, except that higher CD8/CD3 ratios negatively correlated with most other immune cell types (Supporting Fig. S4A).

Infiltration of T cells, Tregs, B cells, plasma cells, $CD11c^+$ dendritic cells (DCs), $S100^+$ DCs, and plasmacytoid DCs (pDCs), and higher Treg/CD4 ratios were histologically associated with poorer differentiation and thicker trabecular patterns (Fig. 1B and Supporting Fig. S4B). The pseudoglandular pattern was significantly associated with lower lymphocytic infiltration. Fibrosis was associated with increased T-cell, B-cell, plasma-cell, and mast-cell infiltration and higher Treg/CD4 ratios, whereas thickened fibrosis (grade 3) tended to be associated with lower lymphocytic infiltration than grade 1/2 fibrosis (Fig. 1B and Supporting Figs. S3 and S4C). Microgranulomas were associated with steatosis and ballooning (Fig. 1B and Supporting Fig. S4D).

Univariate analysis based on the predominant patterns of immune-cell infiltration of each tumor showed that infiltration of $CD4^+$ T cells, $CD8^+$ T cells, total T cells, B cells, plasma cells, and $CD11c^+$ DCs was significantly associated with better prognosis (Fig. 1C,D). To analyze the contribution of heterogeneity of the immune microenvironment, we performed univariate analysis including minor patterns of immune-cell infiltration and found that focal increases in B-cell infiltration were also associated with better prognosis (Fig. 1C). Multivariate analysis showed that B-cell infiltration was the most significant positive prognostic factor among immune cells (Supporting Table S5). Multivariate analysis including B-cell infiltration and conventional histopathological factors also indicated that B-cell infiltration was an independent positive prognostic factor (Supporting Table S6).

DISTINCT IMMUNOSUBTYPES IN HCC REVEALED BY CLUSTER ANALYSIS

We performed cluster analysis of the data derived from the 919 regions to classify patterns within the immune microenvironment. Cluster analysis revealed three distinct patterns of immune-cell infiltration

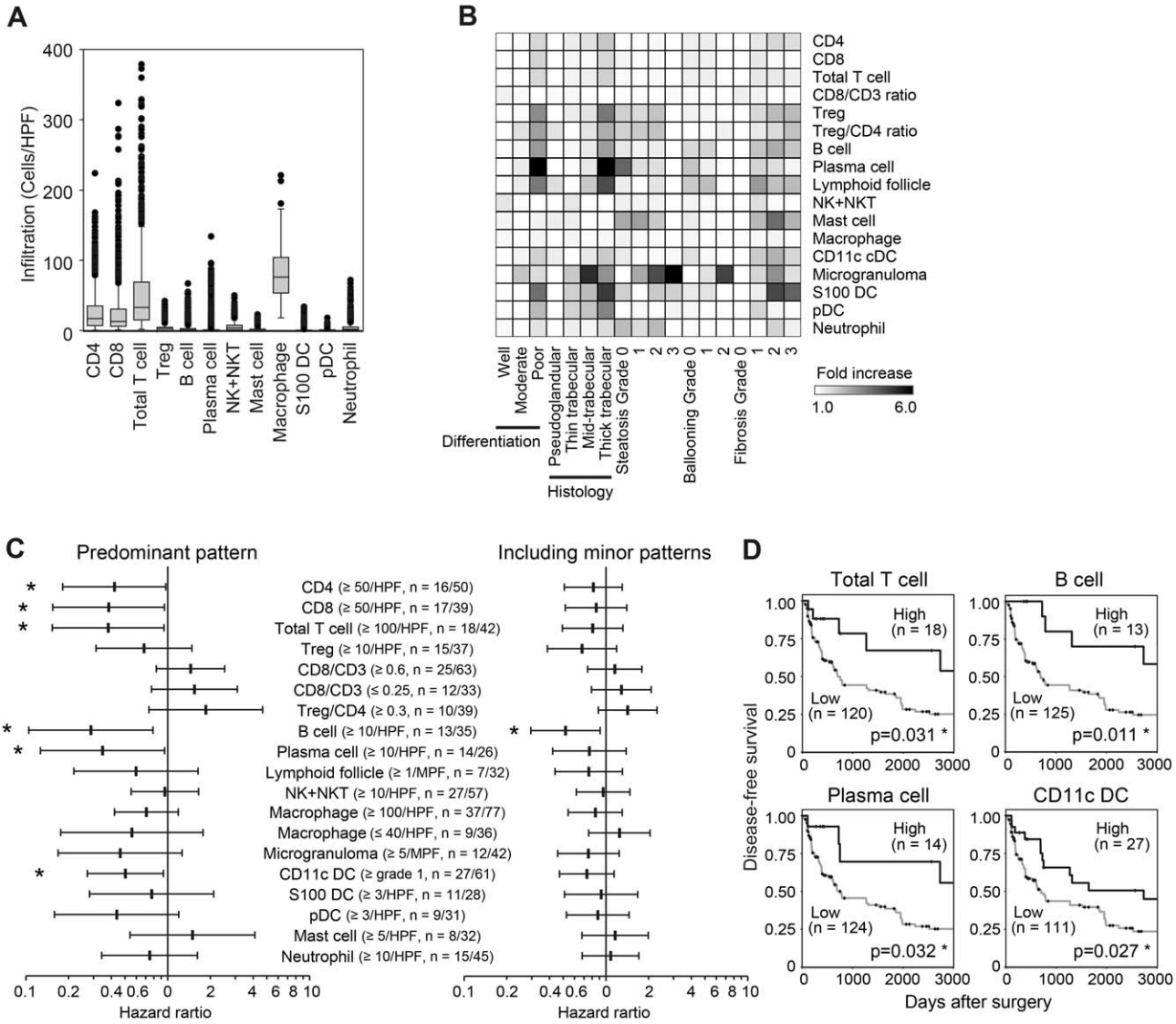

FIG. 1. Adaptive and innate immune-cell infiltration in HCC. (A) Box plot showing the number of infiltrating immune cells in 919 regions. (B) Heat map showing the fold increase (against the lowest value of each line) in immune cells stratified by histopathological factors. (C) Forest plot showing hazard ratios of postsurgical recurrence stratified by the predominant patterns of immune-cell infiltration (left) or by including both predominant/minor patterns of immune-cell infiltration (right). Also indicated are cut-off values and the number of tumors meeting the criteria (n, left: when analyzed in predominant patterns/right: when including both predominant/minor patterns). Total sample size: n = 138. (D) Kaplan-Meyer curve of disease-free survival stratified by the total number of indicated immune cells in predominant patterns with the cut-off values indicated in (C). $^{*}P < 0.05$.

(immunosubtypes): those characterized by increased B-cell, plasma-cell, and T-cell infiltration with variable increases in other immune cell types (Immune-high subtype), moderately increased T-cell and other immune cell infiltration with lesser B- and plasma-cell infiltration (Immune-mid subtype), and low immune-cell infiltration (Immune-low subtype; Fig. 2A). The Immune-mid subtype was subdivided into Immune-mid-1 (a relatively inhomogeneous subtype including regions with increased granuloma formation, mast-cell infiltration, or neutrophil infiltration) and the more homogenous Immune-mid-2 subtype. The Immune-low subtype was also subdivided into those with lower Treg/CD4 ratios (Immune-low-1) and those

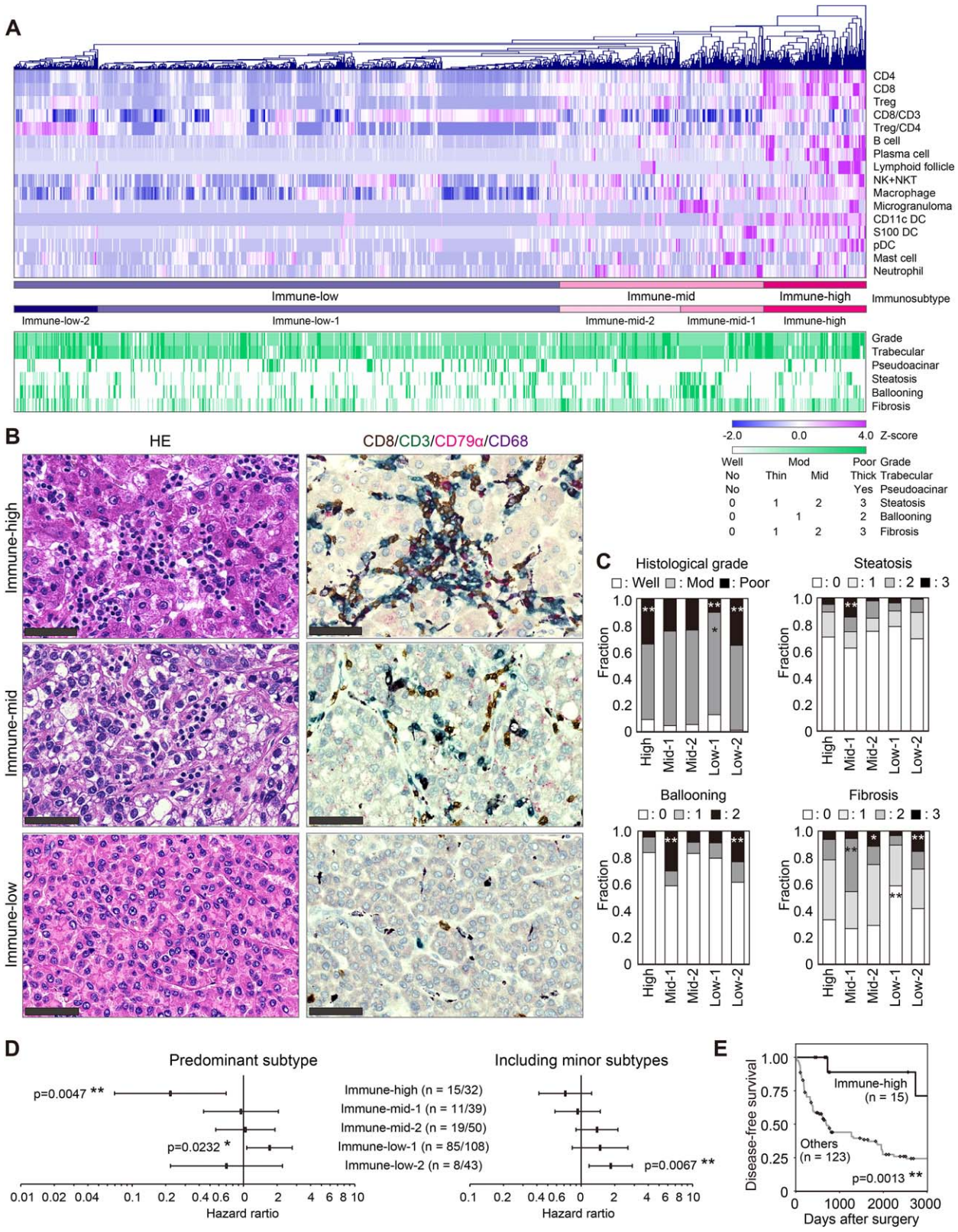

FIG. 2. Cluster analysis showing distinct immunosubtypes in HCC. (A) Heat map showing the results of hierarchical cluster analysis of immune cell infiltration (n = 919). Histopathological findings are indicated in lower panels. (B) Representative histology and multiplex immunohistochemistry of each immunosubtype. Scale bar, 50 μm. HE, hematoxylin and eosin. (C) Bar charts showing associations of immunosubtypes with histopathological findings. (D) Forest plot showing hazard ratios of post-surgical recurrence stratified by predominant subtypes (left) or by including both predominant/minor subtypes (right) of each tumor. Also indicated are the number of tumors belonging to each immunosubtype (n, left: when analyzed in predominant subtypes/right: when including both predominant/minor subtypes). Total sample size: n = 138. (E) Kaplan-Meyer curve of disease-free survival stratified by Immune-high subtype versus other subtypes. $^{*}P < 0.05$; $^{**}P < 0.01$.

characterized by higher Treg/CD4 ratios (Immune-low-2). Representative histological features of the three main immunosubtypes are shown in Fig. 2B.

Among these immunosubtypes, the Immune-high and Immune-low-2 subtypes were significantly associated with poorly differentiated regions, whereas Immune-low-1 subtype was significantly less associated with poorly differentiated regions (Fig. 2C). The Immune-mid-1 subtype was significantly associated with steatosis and ballooning because it included a microgranuloma-high subpopulation. Fibrosis was significantly associated with Immune-mid and Immune-low-2 subtypes, while significantly less associated with the Immune-low-1 subtype (Fig. 2C). Interestingly, the Immune-high subtype showed significantly less intratumor arterial vessel density analyzed by h-caldesmon IHC (Supporting Fig. S5), indicating impaired arterial tumor-vessel formation and different hemodynamic status between Immune-high and non-Immune-high HCCs.

PROGNOSTIC SIGNIFICANCE OF IMMUNOSUBTYPES AND INTRATUMOR HETEROGENEITY

Univariate analysis based on predominant immunosubtypes showed Immune-high–predominant HCC to be significantly associated with better prognosis and Immune-low-1–predominant HCC to be associated with poorer prognosis (Fig. 2D,E). The prognosis of Immune-low-2–predominant HCC remained unclear because of small sample size (n = 8). There were no significant etiological differences between HCCs with each predominant immunosubtype (Supporting Fig. S6A). Immune-high–predominant HCCs were significantly associated with lower grade of fibrosis in the background liver (Supporting Fig. S6A).

Regarding intratumor heterogeneity of the immune microenvironment, more than 50% of each immunosubtype-predominant HCC contained more than one immunosubtype (Supporting Fig. S6B). Univariate analysis including minor immunosubtypes showed the existence of focal Immune-low-2 component to be associated with poorer prognosis (Fig. 2D). The focal appearance of Immune-low-2 subtype was mainly observed in Immune-mid-2– and Immune-low-1–predominant HCCs, but failed to show prognostic significance in these HCCs (Supporting Fig. S6C,D).

Multivariate analysis revealed that the Immune-high subtype was an independent positive prognostic factor (Supporting Table S7), whereas the Immune-low-1 subtype and focal appearance of Immune-low-2 subtype were not. Most tumors belonging to the Immune-high–predominant subtype overlapped with those with combined infiltration of T, B, and plasma cells (Supporting Fig. S7). Therefore, IHC evaluation of $CD3^+$ T cell and $CD79\alpha^+$ B/plasma cells can serve as a surrogate marker for the classification of the Immune-high subtype.

We also analyzed immune-cell infiltration at the interface between HCC and background liver tissue. Significantly higher infiltration of T, B, and plasma cells to the interface region was observed in Immune-high–predominant HCCs and also associated with better prognosis (Supporting Fig. S8A,B). Grade of fibrosis in background liver tissue did not affect the amount of immune-cell infiltration at the interface region (Supporting Fig. S8C).

ADDITIONAL PROGNOSTIC IMPACT OF IMMUNOSUBTYPES ON HISTOPATHOLOGICAL AND MOLECULAR CLASSIFICATIONS OF HCC

We next compared immunosubtypes with histological and molecular classification of HCC.[21-23] Histological grade of HCC showed borderline prognostic significance (Supporting Table S2; Fig. 3A). Immune-high–predominant HCC constituted around 25% of poorly differentiated HCCs and showed significantly better prognosis among poorly differentiated HCCs. Well- to moderately differentiated HCC mainly constituted of Immune-low–predominant HCC, and stratification by immunosubtype showed no prognostic value.

IHC-based molecular classification of HCC has shown that cytokeratin 19 (CK19) and/or Sal-like protein 4 (SALL4) positivity forms a subgroup of HCC with poorer prognosis (biliary/stem-1 subclass).[23] Whereas expression of epithelial cell adhesion molecule (EpCAM) is also considered to represent stem-like features, EpCAM expression without biliary/stem-1 marker expression is not a significant prognostic indicator (biliary/stem-2 subclass).[23] Nuclear β-catenin localization and/or diffuse glutamine synthetase (GS) expression is associated with Wnt/β-catenin activation (Wnt/β-catenin subclass). This IHC-based

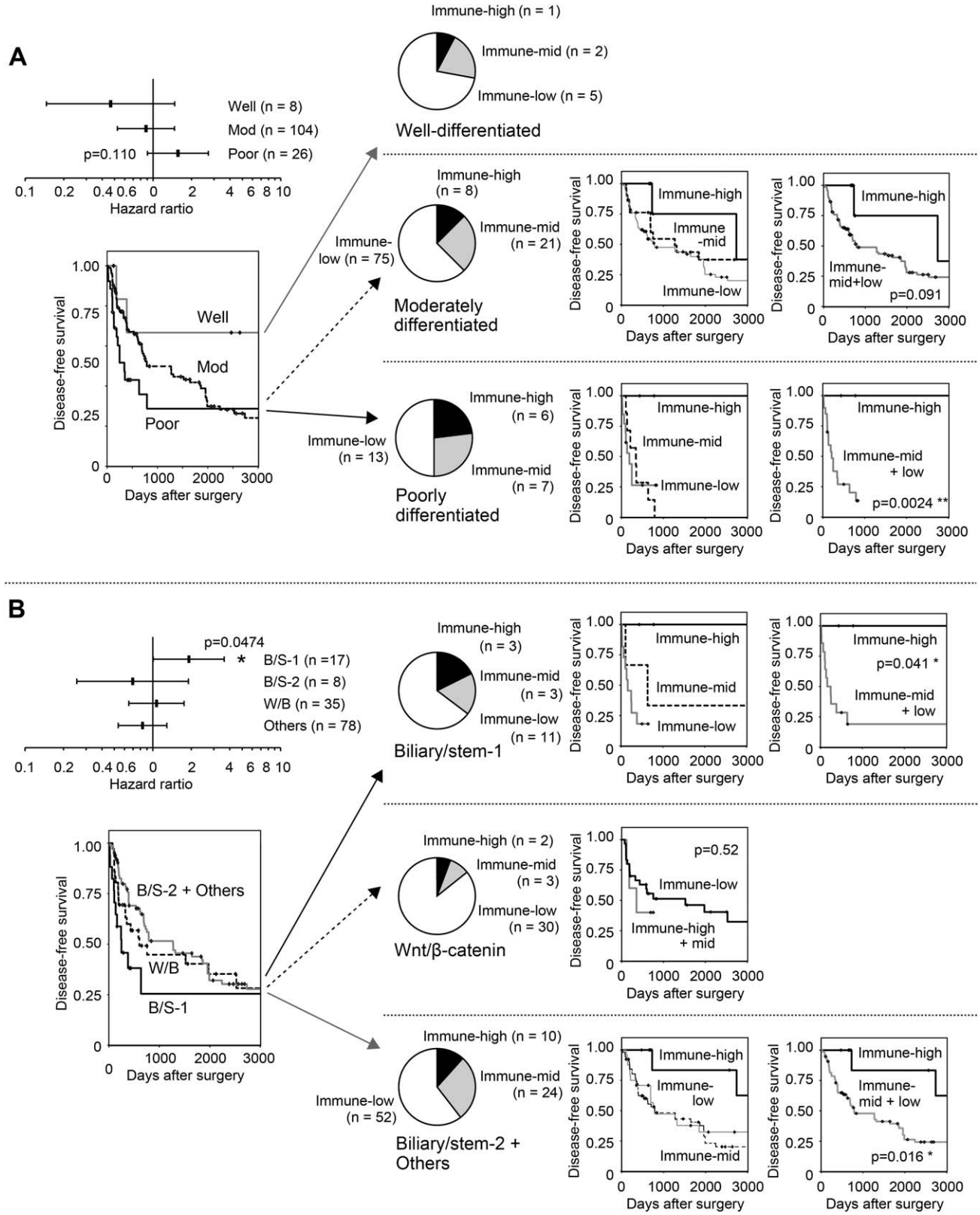

FIG. 3. Additional prognostic impact of immunosubtypes on histopathological and IHC-based molecular classifications of HCC. (A) (Left upper) Forest plot showing hazard ratios of postsurgical recurrence stratified by the HCC histological grade. Total sample size: n = 138. (Left lower) Kaplan-Meyer curve of disease-free survival (DFS) stratified by histological grade of HCC. (Middle) Pie charts showing the fractions of immunosubtypes in each HCC grade. (Right) Kaplan-Meyer curves of DFS of each HCC grade stratified by immunosubtypes. (B) (Left upper) Forest plot showing hazard ratios of postsurgical recurrence stratified by IHC-based molecular subclass of HCC. Total sample size: n = 138. (Left lower) Kaplan-Meyer curves of DFS stratified by molecular subclass. (Middle) Pie charts showing the fractions of immunosubtypes in each molecular subclass. (Right) Kaplan-Meyer curves of DFS of each molecular subclass stratified by immunosubtypes. $^{*}P < 0.05$; $^{**}P < 0.01$.

molecular classification of HCC showed weak prognostic significance (Supporting Table S2; Fig. 3B). Immune-high–predominant HCC constituted nearly 20% of the biliary/stem-1 subclass and around 10% of non-biliary-stem-1 and non-Wnt/β-catenin subclasses and showed significantly better prognosis in these subclasses. On the other hand, only a small number of Immune-high– and Immune-mid–predominant HCCs were observed in the Wnt/β-catenin subclass, and immunosubtypes had no prognostic values in the Wnt/β-catenin subclass. Therefore, evaluation of immune cells in HCC offers additional clinicopathological significance on top of the conventional histopathological and molecular classifications. Similar results were obtained when cases were stratified by B- and plasma-cell infiltration (Supporting Fig. S9).

We also compared immunosubtypes with Hoshida's 30-gene signature (S1, S2, and S3)[24,25] and Boyault's 16-gene signature (G1 to G6)[26] in 154 regions of 40 HCCs with region-matched cDNA samples (Fig. 4A). In the current cohort, Hoshida's S2 was enriched with Boyault's G1 and CK19$^+$/SALL4$^+$/EpCAM$^+$ HCCs, whereas Hoshida's S3 was enriched with Boyault's G5/6 and β-catenin$^+$/GS$^+$ HCCs (Fig. 4A,B). These results were compatible with previous studies.[21] Hoshida's S1 and Boyault's G2 were significantly associated with the Immune-high subtype and Hoshida's S3 and Boyault's G6 with the Immune-low subtype (Fig. 4C). Interestingly, among the "proliferative phenotype" HCCs (Hoshida's S1/2 and Boyault's G1 to G3),[21] the Immune-high subtype was observed in Boyault's G2/3, but not in Boyault's G1. These differences may also have impact on the clinical course of HCC; however, we could not perform prognostic analysis using these data because of small sample size (n = 40) and shorter follow-up period (these samples were obtained between 2016 and 2017).

IMMUNOSUBTYPES AND LYMPHOCYTE-RICH, LYMPHOEPITHELIOMA-LIKE, AND STEATOHEPATITIC HCC

There are two histological entities associated with immune-cell infiltration in HCC: lymphoepithelioma-

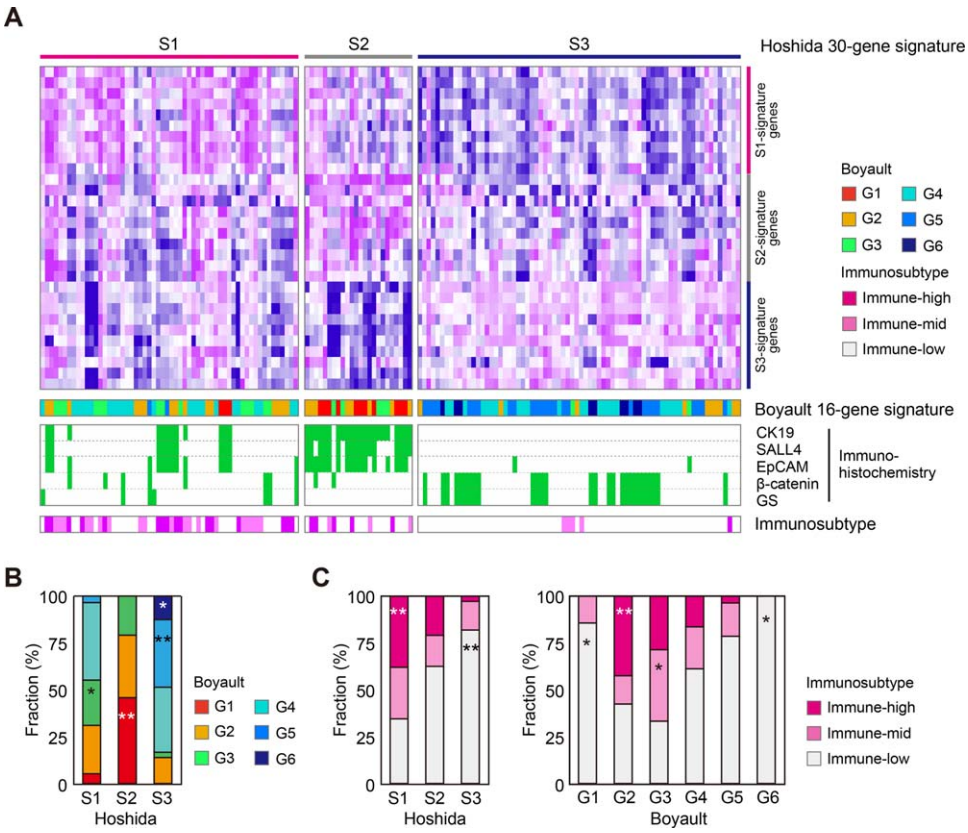

FIG. 4. Immunosubtypes and Hoshida's/Boyault's molecular classification of HCC. (A) Heat map showing the results of k-means cluster analysis (k = 3) of Hoshida's 30-gene signature using mRNA samples from 154 regions of 40 HCCs. Corresponding results of Boyault's 16-gene signature, region-matched findings of IHC, and region-matched immunosubtypes are shown in lower panels. (B) Bar chart showing the fraction of Boyault's 16-gene signature in each Hoshida's 30-gene signature. (C) Bar charts showing the fraction of immunosubtypes in each Hoshida's 30-gene signature (left) and Boyault's 16-gene signature (right). $^*P < 0.05$; $^{**}P < 0.01$.

like and steatohepatitic HCC. Given that the definition of lymphoepithelioma-like HCC is unclear,[27] we defined lymphocyte-rich HCC as having ≥100 cells/high-power field (HPF) T-cell infiltrations in predominant regions in accord with Wada's definition,[12] and we defined lymphoepithelioma-like HCC as lymphocyte-rich HCC with massive lymphocytic infiltration into the tumor nest. We adopted the recent definition of steatohepatitic HCC.[28] Representative histology is shown in Fig. 5A.

As defined above, lymphoepithelioma-like, lymphocyte-rich, and steatohepatitic HCCs were found in 2.89%, 10.1%, and 9.42%, respectively, of 138 HCCs. There were no significant etiological differences (Supporting Fig. S10A). Significant increases in T-cell, B-cell, and plasma-cell infiltration were observed in steatohepatitic, lymphocyte-rich, and lymphoepithelioma-like regions in that order (Fig. 5B,C). Immune-high–predominant HCC constituted 75% and 57% of lymphoepithelioma-like and lymphocyte-rich HCC, respectively. Lymphoepithelioma-like and lymphocyte-rich HCCs with the Immune-high subtype tended to have better prognosis, although not statistically significant because of the limited sample size (Supporting Fig. S10B).

CHANGES IN THE IMMUNE MICROENVIRONMENT DURING MULTISTEP CARCINOGENESIS

To analyze changes in the immune microenvironment during tumor progression, we compared immune-cell infiltration between regions with different histological grades in the same tumor. Twenty-three of 158 tumors (14.5%) showed histological transition from well-differentiated to moderately differentiated regions, in which significant decreases in the CD8/CD3 ratio and in $CD56^+$ NK/NKT cell and macrophage infiltration were observed (Fig. 5D). Sixteen of 158 tumors (10.1%) showed transition from moderately differentiated to poorly differentiated regions, in which a significant increase in Treg infiltration, but not in Treg/CD4 ratio, was observed (Fig. 5E). T-cell infiltration increased or decreased on a case-by-case basis during the transition from moderately differentiated to poorly differentiated regions (Fig. 5E), which was compatible with the observation that poorly differentiated HCCs were associated with two opposite immunosubtypes, namely, Immune-high and Immune-low-2 subtypes (Figs. 2C and 3A).

ASSOCIATION OF Immune-high SUBTYPE WITH TYPE 1 T HELPER/CYTOTOXIC T LYMPHOCYTE–TYPE CYTOKINE/CHEMOKINE MILIEU

To analyze the cytokine and chemokine milieu characterizing each HCC immunosubtype, we analyzed the expression of selected cytokine and chemokine mRNAs in 80 regions of 21 HCCs (Fig. 5A). We analyzed *Ifng, Gzmb, Cxcl9, Cxcl10, Il12a, Il12b, Il27*, and *Tnfa* as type 1 T helper (Th1)/cytotoxic T lymphocyte (CTL)-related transcripts; *Il17a, Il17f, Il23r*, and *Il23a* as Th17-related transcripts; *Ccl20, Ccl22, Il10*, and *Ebi3* as Treg/immunoregulatory transcripts; *Cxcl12* as fibroblast-related transcript; and *Ccr2, Cx3cl1*, and *Il6* as macrophage-related transcripts. Hierarchical cluster analysis showed regions with high expression of Th1/CTL-related mRNA (especially *Ifng, Gzmb, Cxcl9*, and *Cxcl10*; Fig. 6A), which was very similar to the previously defined "Immune class" signature in HCC.[5] Expression of Th17-related mRNA was relatively low, which is compatible with a previous study showing a lower frequency of Th17 cells among tumor-infiltrating lymphocytes in HCC.[29] Th1/CTL-type cytokine/chemokine milieu was associated with increased T-, B-, and plasma-cell infiltration and the Immune-high subtype (Fig. 6A-C).

Because chemokine (C-X-C motif) ligand (CXCL)10 is a key chemokine in recruiting immune cells[11,30] and promotes plasma-cell differentiation from B cells,[31] we sought to identify the sources of CXCL10 in tumor tissue. IHC analysis showed clear CXCL10 positivity in *Cxcl10* mRNA-high HCC, but not in *Cxcl10* mRNA-low HCC (Fig. 6D). Moreover, CXCL10 was mainly produced by $CK18^+$ tumor cells (Fig. 6E). Tumor cells were not found to be diffusely positive for CXCL10; rather, they tended to express CXCL10 at the interface with leukocytic infiltration (Fig. 6D).

Given that this Th1/CTL-related cytokine/chemokine milieu in Immune-high subtype could potentially affect macrophage polarization, we analyzed phenotypes of macrophages in each immunosubtype. According to previous studies,[32,33] we observed that more than 90% of tumor-associated macrophages expressed M2 marker CD163 and CD204 (Supporting Fig. S11). Another study has shown that intratumor $CD169^+$ macrophages can stimulate T cells and are associated with better prognosis in HCC.[34]

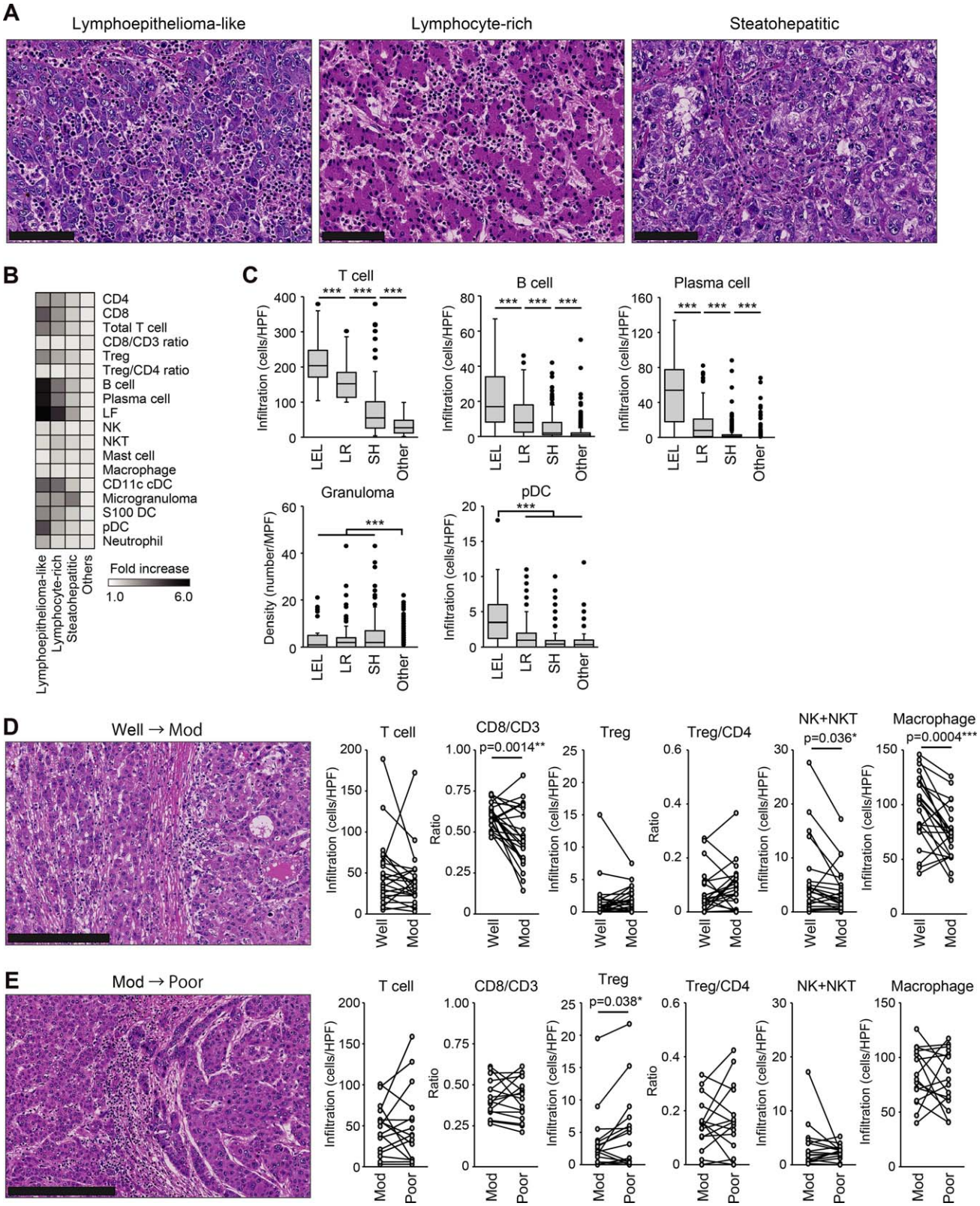

FIG. 5. Immune microenvironment in lymphoepithelioma-like, lymphocyte-rich, and steatohepatitic HCC and changes during multistep carcinogenesis of HCC. (A) Representative histology showing lymphoepithelioma-like, lymphocyte-rich, and steatohepatitic HCC. Scale bar, 100 μm. (B) Heat map showing the fold increase (against the lowest value of each line) in immune cells stratified by histology. (C) Box plots showing the numbers of infiltrated immune cells (LEL, lymphoepithelioma-like, n = 38; LR, lymphocyte-rich, n = 133; SH, steatohepatitic, n = 121; others, n = 553). (D) (Left) Representative histology showing the transition from well-differentiated (Well) to moderately differentiated (Mod) regions. Scale bar, 250 μm. (Right) Line graphs showing changes in the numbers of immune cells from well-differentiated to moderately differentiated regions (n = 23). (E) (Left) Representative histology showing the transition from moderately (Mod) to poorly differentiated (Poor) regions. Scale bar, 250 μm. (Right) Line graphs showing changes in the numbers of immune cells from moderately differentiated to poorly differentiated regions (n = 16). $^{*}P < 0.05$; $^{**}P < 0.01$; $^{***}P < 0.001$.

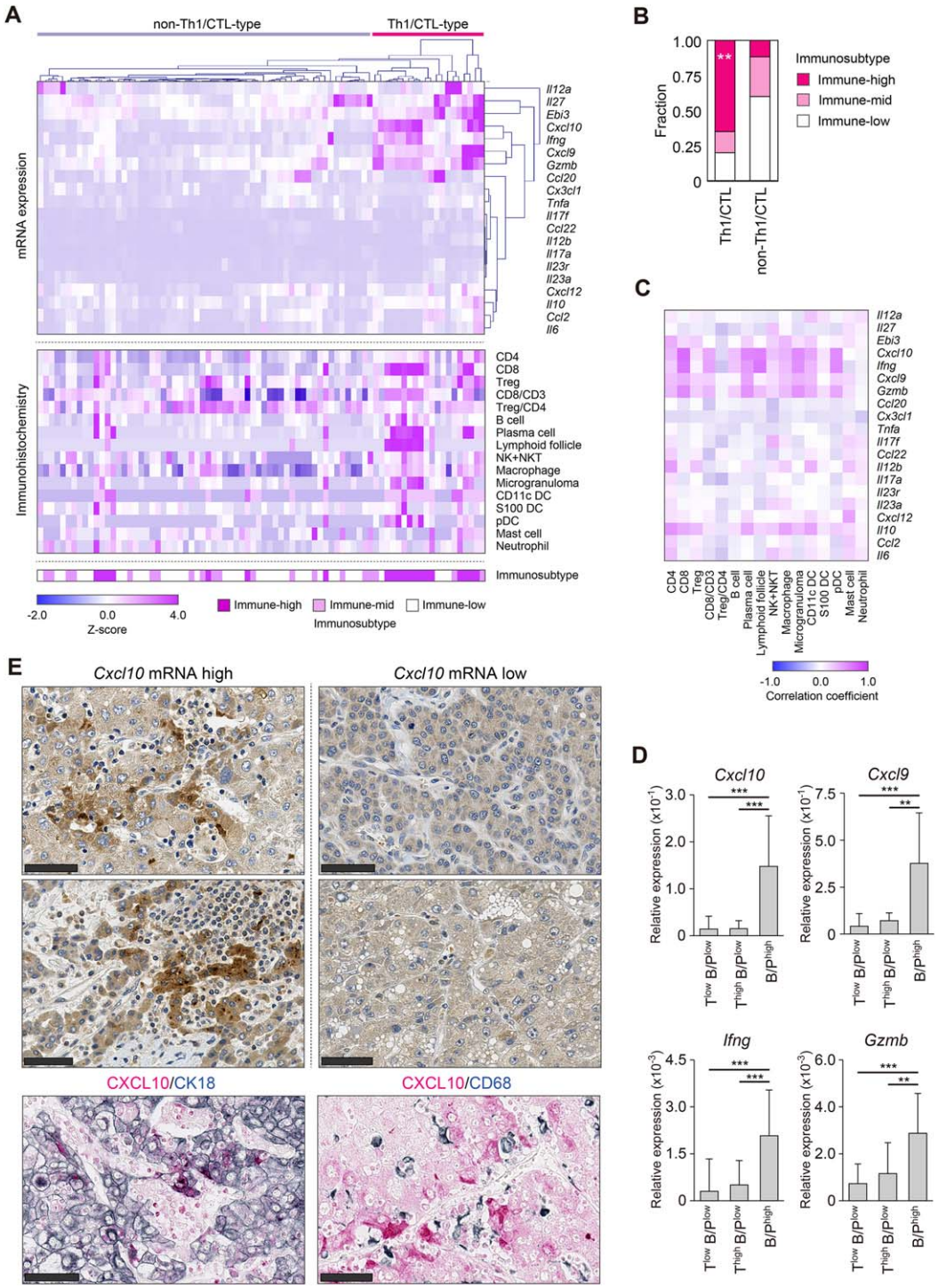

FIG. 6. Immune microenvironment and local cytokine/chemokine milieu. (A) Heat map showing the results of hierarchical cluster analysis of cytokine/chemokine mRNA expression in 80 regions of 21 HCCs (top). Corresponding patterns of immune-cell infiltration (middle) and immunosubtypes (bottom) are also indicated. (B) Bar chart showing the fraction of immunosubtypes in each cytokine/chemokine milieu analyzed in (A). (C) Heat map showing correlation coefficients between cytokine/chemokine mRNA expression and immune-cell infiltration. (D) Bar charts showing indicated mRNA expression in regions with particular immune microenvironments (T^{low}: T-cell infiltration < 50 cells/HPF, T^{high}: ≥ 50 cells/HPF, B/P^{low}: both B- and plasma-cell infiltration < 10 cells/HPF, B/P^{high}: B- and/or plasma-cell infiltration ≥ 10 cells/HPF, $T^{low}B/P^{low}$: n = 42, $T^{high}B/P^{low}$: n = 17, B/P^{high}: n = 21). (E) (Top) Representative IHC of CXCL10 in cases with high and low expression of *Cxcl10* mRNA analyzed in (A) (representative results of each, n = 5). (Bottom) Representative double IHC of CXCL10/CK18 (left) and CXCL10/CD68 (right) in cases with high expression of *Cxcl10* mRNA analyzed in (A) (representative results of each, n = 5). Scale bar, 50 μm. $^{**}P < 0.01$; $^{***}P < 0.001$.

Consistently, we observed increased fraction of $CD169^+$ macrophages in the Immune-high subtype (Supporting Fig. S11).

IMMUNOSUBTYPES AND PROGRAMMED DEATH LIGAND 1/PROGRAMMED DEATH 1 EXPRESSION

We analyzed programmed death ligand 1 (PD-L1)/programmed death 1 (PD1) expression and compared the results with immunosubtypes in selected cases (n = 64). Consistent with a previous study,[35] we observed PD-L1 expression in tumor cells and clusters of immune cells (Fig. 7A). The majority of $PD\text{-}L1^+$ immune cells were $CD68^+$ macrophages (Fig. 7B). Expression of PD-L1 in both tumor and immune cells were significantly associated with the Immune-high subtype (Fig. 7C). Consistent with the association of PD-L1 positivity with Immune-high subtypes, PD-L1 expression in tumor cells and immune cells was associated with better prognosis (Supporting Fig. S12).

PD1 expression was observed in inflammatory cells, of which the majority was $CD8^+$ T cell (Fig. 7D). PD1 positivity in $CD8^+$ T cells was also associated with the Immune-high subtype (Fig. 7D). Although it was not significantly associated with PD-L1 positivity in tumor cells, PD1 positivity in $CD8^+$ T cells was significantly associated with PD-L1 and CD169 positivity in macrophages (Fig. 7E), indicating the coexistence of complex stimulatory/inhibitory interactions between infiltrating $CD8^+$ T cells and macrophages in the Immune-high subtype microenvironment.

IMMUNOSUPPRESSIVE PHENOTYPE OF INFILTRATING PLASMA CELLS

Although increased B- and plasma-cell infiltration is associated with Th1/CTL-type immune reaction and improved prognosis, functional analysis of B and plasma cells in murine studies have indicated their immunosuppressive roles through the alternate expression of interleukin (IL)-10 and IL-35 (heterodimer of IL-12A/p35 and Epstein Barr virus-induced gene 3 [EBI3]) during the differentiation of activated B cells into plasmablasts and plasma cells.[36,37] B and plasma cells can also inhibit tumor immunity through immunoglobulin-mediated alternative activation of macrophages.[38]

In HCC, expressions of *Il10* and *Ebi3* mRNA were significantly associated with B-/plasma-cell infiltration, whereas expressions of *Il12a* (encoding IL-12a/p35) and *Il27* (encoding the p28 subunit forming IL-27 together with EBI3) were not significantly associated with B-/plasma-cell infiltration (Supporting Fig. S13A). IHC analysis of IL-10 revealed it to be mainly positive in tumor cells in *Il10* mRNA-high, but not in *Il10* mRNA-low tumors (Supporting Fig. S13B), suggesting that IL-10 was mainly produced by tumor cells, not by lymphocytes including B cells. IHC analysis of EBI3 expression also showed correlation of IHC results with *Ebi3* mRNA expression (Supporting Fig. S13C). In addition to tumor cells, EBI3 expression was also clearly observed in stromal cells (Supporting Fig. S13C), as observed.[39] These stromal cells were mainly $CD20^-CD79\alpha^+$ plasma cells, but a small fraction of $CD20^+$ B cells also expressed EBI3 (Supporting Fig. S13D). These results strongly indicate that plasma cells are a major source of IL-35 and highlight their possible immunosuppressive roles in the HCC microenvironment.

Discussion

The most striking results from the current comprehensive analysis of the HCC immune microenvironment were that the immune microenvironment can be classified into three major distinct immunosubtypes (Immune-high, Immune-mid, and Immune-low). The Immune-high subtype is characteristically associated with increased B-/plasma-cell infiltration, and the Immune-high subtype and B-cell infiltration are the most significant independent positive prognostic factors among immune-related variables. Although considerable intratumor heterogeneity of the immune microenvironment was observed in some HCCs, the predominant immunosubtype in each tumor was prognostically important.

The prognostic roles of B-/plasma-cell infiltration in HCC have been controversial. Some studies have shown that chemokine-driven T- and B-cell infiltrations are associated with better prognosis,[16,17] whereas another study indicated that B-cell infiltration is associated with IL-17 production and poorer prognosis.[15] In a current study, we have shown that the Immune-high subtype characterized by coinfiltration of T and B/plasma cells is an independent positive prognostic factor. Importantly, the Immune-high subtype indicates HCCs with better prognosis among

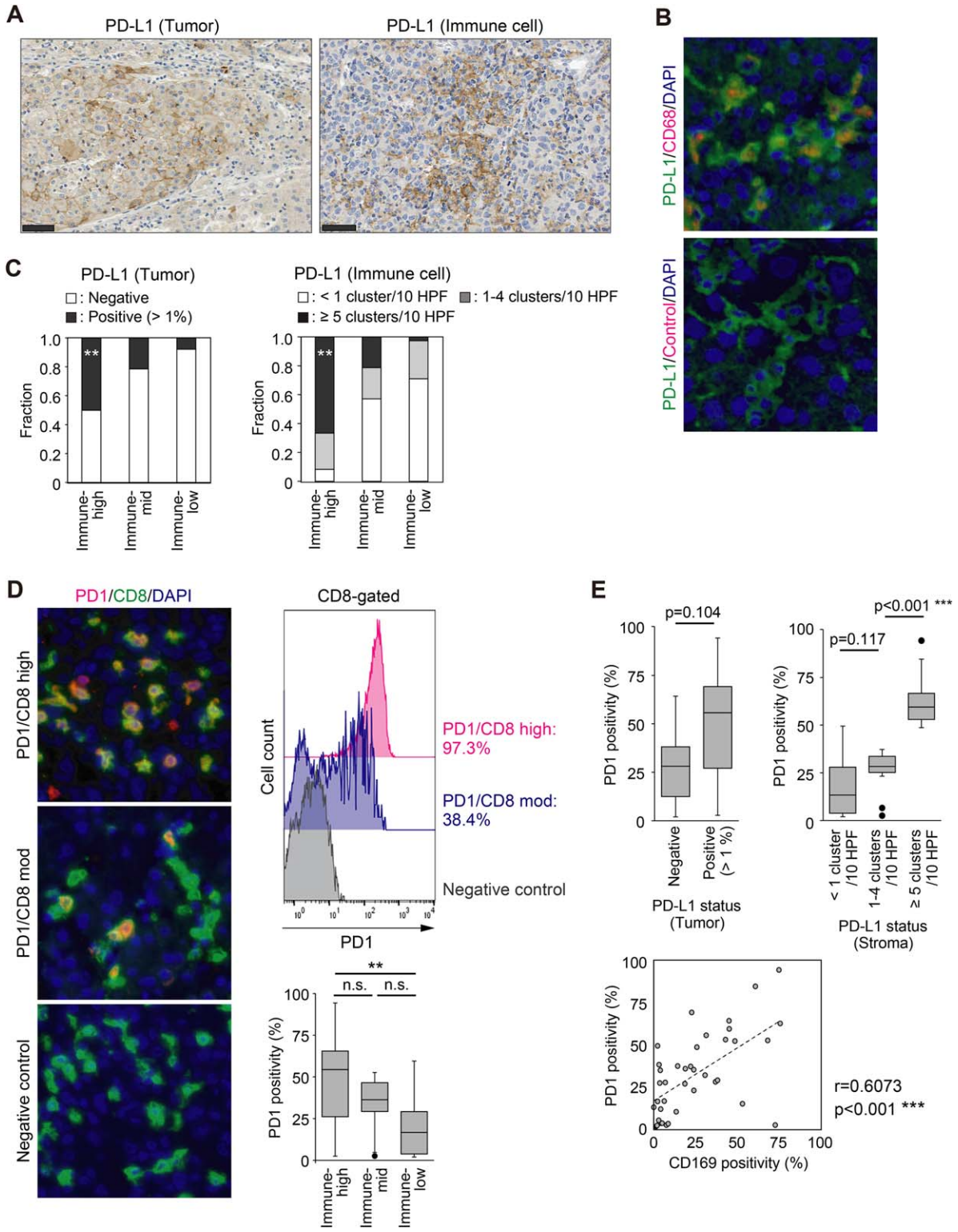

FIG. 7. Immunosubtype and PD-L1/PD1 expression. (A) Representative IHC of PD-L1 in tumor (left) and in immune cells (right). Scale bar, 50 μm. (B) Fluorescent IHC of PD-L1 (green), CD68 (red), and DAPI (blue). Representative figures of five independent experiments are shown. (C) Bar charts showing the associations of immunosubtypes with PD-L1 expression by tumor (left) and immune cells (right). Immune-high, n = 12; Immune-mid, n = 14; Immune-low, n = 38. (D) (Left) Fluorescent IHC of PD1 (red), CD8 (green), and DAPI (blue). (Right upper) Histogram of PD1 expression in $CD8^+$ T cells. (Right lower) Box plot showing PD1 positivity in $CD8^+$ T cells stratified by immunosubtypes. Immune-high, n = 12; Immune-mid, n = 14; Immune-low, n = 38. (E) (Left upper) Box plot showing PD1 positivity in $CD8^+$ T cells stratified by PD-L1 status in tumor cells (negative, n = 52; positive, n = 12). (Right upper) Box plot showing PD1 positivity in $CD8^+$ T cells stratified by PD-L1 status in immune cells (< 1 cluster/10HPF, n = 36; 1-4 clusters/10HPF, n = 16; ≥ 5 clusters/10HPF, n = 12). (Lower) Dot plot showing correlation of PD1 positivity in $CD8^+$ T cells and CD169 positivity in macrophages (n = 64). $^*P < 0.05$; $^{**}P < 0.01$; $^{***}P < 0.001$.

poorly differentiated HCCs and CK19$^+$ and/or SALL4$^+$ high-grade HCCs,[21,23] whereas the immunosubtypes were not prognostically significant in well- to moderately differentiated HCCs and Wnt/β-catenin HCC. Therefore, the prognostic impacts of the immune microenvironment differ among the histopathological/molecular tumor subclasses. These results provide a rationale for the pathological evaluation of the immune microenvironment in addition to the current histopathological and molecular classifications of HCC. We also showed that lymphoepithelioma-like[27] and lymphocyte-rich HCCs[12] with the Immune-high subtype tend to have better prognosis than those with the non-Immune-high subtype, indicating that not only the amount and lymphoepithelioma-like pattern of lymphocyte infiltration, but also the component of these lymphocytes (coinfiltration of T and B/plasma cells) reflect the activity of immune reaction against tumors. Further characterization of the phenotype and function of infiltrating T, B, and plasma cells in Immune-high, lymphoepithelioma-like, and lymphocyte-rich HCCs would be important to understand the patterns of active immune reaction against HCCs.

Histopathological analysis of the immune microenvironment facilitated investigation of how the immune microenvironment changes during focal progression of HCC. We found that decreases in the CD8/CD3 ratio and CD56$^+$ NK-/NKT-cell infiltration first occur during the development from well-differentiated to moderately differentiated HCC, with total T-cell infiltration not significantly changed. T-cell infiltration increases or decreases (depending on the tumor) more clearly during the development from moderately differentiated to poorly differentiated HCC, which is compatible with our finding that poorly differentiated HCC is associated with two contrasting immunosubtypes: Immune-high and Immune-low subtypes. Evidently, the immune microenvironment does not change in a linear manner, but changes in a multistep process associated with the multistep carcinogenesis of HCC.[18]

The mechanism of the development of different immune microenvironments needs to be clarified. There were no significant etiological differences between immunosubtypes. On the other hand, Immune-high–predominant HCC was significantly associated with the lower grade of fibrosis in the background liver. This may indicate that the preexisting immunosuppressive microenvironment in cirrhotic or precirrhotic liver[40] has some involvement in the formation of the Immune-low microenvironment in HCCs.

We have also shown the associations of immunosubtypes and previously established molecular subclasses of HCC (Hoshida's 30-gene signature and Boyault's 16-gene signature).[24-26] The Immune-high subtype was significantly enriched in Hoshida's S1 and Boyault's G2 subclasses, with the Immune-low subtype in Hoshida's S3 and Boyault's G6 subclasses. Interestingly, none of the Immune-high subtype was observed in Boyault's G1 subclass among the "proliferative phenotype" HCCs (composed of Hoshida's S1/S2 and Boyault's G1 to G3).[21] These results indicate the importance of molecular mechanisms shaping these transcriptome-based classifications of HCC in modulating immune reaction against tumors. Actually, studies have shown that the tumor-intrinsic activation of specific signaling pathways can affect immune-cell infiltration. In HCC, mutations of *CTNNB1* (associated with Hoshida's S3 and Boyault's G5/6 subclasses) and *TP53* (associated with Hoshida's S1/2 and Boyault's G1 to G3 subclasses) are major mutations,[22] and recent comprehensive molecular analysis revealed associations between *CTNNB1* mutation, and lower lymphocytic infiltration[5,41] as confirmed in the current study. Mechanistically, in melanoma, *CTNNB1* mutation decreases the recruitment of proinflammatory DCs and T cells through decreased chemokine CCL4 expression.[42] Gene mutations other than those of *CTNNB1* are not currently linked to specific immune microenvironments in HCC.[5]

CXCL9 and CXCL10 expressions are associated with lymphocytic infiltration in many tumors.[16,30] We found that the Immune-high subtype is characterized by a CXCL9/CXCL10-rich Th1/CTL-type cytokine/cytokine milieu, which is similar to "Immune class" as defined by the gene-expression–based approach.[5] We also found that CXCL10 is mainly produced by tumor cells. It is unclear whether CXCL10 is expressed in HCC in a tumor-cell–intrinsic manner or is induced by interferon-γ–rich lymphocytic stroma. However, the distribution of CXCL10-expressing tumor cells at the interface with B-/plasma-cell–rich immune microenvironments may indicate the latter possibility; therefore, the molecular mechanisms behind the formation of the Immune-high subtype HCC is still largely unclear and require further research.

In addition to the findings for CXCL10, we observed that PD-L1 expressions in tumor and immune cells (mainly macrophages) are associated

with the Immune-high subtype, which is consistent with a recent study showing the relationship between PD-L1 expression and the "Immune class" as defined by Zhou et al.[5] We also observed that PD1 positivity in $CD8^+$ T cells is associated with the Immune-high subtype. Intriguingly, PD1 positivity in $CD8^+$ T cells is significantly associated with PD-L1 expression in macrophages rather than those in tumor cells. Given that the expression of PD-L1 in tumor cells is often very focal in HCC, these data indicate tumor-infiltrating macrophage as a main partner of PD1/PD-L1–mediated interaction with $CD8^+$ T cells. On the other hand, we also found that macrophages in the Immune-high subtype are also associated with CD169 positivity, an indicator for M1-like phenotype and their ability to stimulate T cells.[34] Therefore, complex stimulatory/inhibitory interactions may coexist between infiltrating $CD8^+$ T cells and macrophages in Immune-high subtype HCC.

Although B-/plasma-cell infiltration in HCC is associated with the Immune-high subtype and better prognosis, the role of B/plasma cells in the immune microenvironment is still unclear. Plasma cells can produce large amounts of antigen-specific immunoglobulins; however, immunoglobulins may contribute to the formation of tumor-supporting microenvironments by inducing alternative activation of macrophages through Fc receptors.[38] B/plasma cells can also play immunosuppressive roles through the alternate expression of IL-10 and IL-35 during differentiation of activated B cells into plasmablasts and plasma cells.[36,37] In the current study, we found that IL-10 is mainly produced by tumor cells and that B/plasma cells are not the main producer of IL-10 in HCC. However, expression of IL-35, analyzed as EBI3 positivity, was clearly observed in $CD20^-CD79\alpha^+$ plasma cells in addition to tumor cells. Because EBI3 expression is a late-limiting process of IL-35 production, with basal expression of its heterodimeric partner (IL-12A/p35) in plasma cells,[36] we suggest that plasma cells are a major source of IL-35 in HCC. These results indicate that complex anti- and protumor interactions also coexist around the infiltrating B/plasma cells in Immune-high HCC, and further characterization of the phenotypes and functions of B/plasma cells in human tumors is required.

There are several limitations in this study. First, because the HCC cohort in the current study does not contain the cases with neoadjuvant therapies using immune-checkpoint inhibitors and kinase inhibitors (e.g., sorafenib), we could not analyze the effect of these therapeutics to the immune microenvironment. Second, the HCC cohort in the current study is composed of surgically resected HCCs and does not contain cases with advanced HCC, which are more common as a target of immune-checkpoint inhibitors. Future studies including biopsy samples from advanced HCCs and/or autopsy cases will overcome this limitation. Third, although we have shown the association of immunosubtypes with Hoshida's and Boyault's molecular classification of HCC, we could not perform additional prognostic analysis because of the shorter follow-up period in these HCC cohorts with matched mRNA samples. The molecular mechanisms to form different immunosubtypes are also still largely unclear, and further researches are required. Fourth, although we have shown the possible immunosuppressive effect of tumor-infiltrating plasma cells by producing IL-35, we could not perform the functional analysis of these plasma cells because of the small numbers of plasma-cell–rich (Immune-high subtype) HCCs. Further research is required to determine whether these plasma cells are immunosuppressive and could be a new target of immunotherapy against HCC.

In conclusion, we have shown that the immune microenvironment of HCC can be classified into three immunosubtypes (Immune-high, Immune-mid, and Immune-low) with additional prognostic impact on histological and molecular classification of HCC. The Immune-high subtype is associated with poorly differentiated HCC, constitutes about 20% of $CK19^+$ and/or $SALL4^+$ high-grade HCC, and shows significantly better prognosis in these high-grade HCCs. The Immune-high subtype is also characterized by its association with Hoshida's S1/Boyault's G2 molecular subclasses, Th1/CTL-type cytokine/chemokine milieu, and increased PD1/PD-L1 positivity in $CD8^+$ T cells, macrophages, and tumor cells. We also observed that these immune microenvironments in HCC change during the course of multistep carcinogenesis.

REFERENCES

1) Hanahan D, Coussens LM. Accessories to the crime: functions of cells recruited to the tumor microenvironment. Cancer Cell 2012;21:309-322.
2) Palucka AK, Coussens LM. The basis of oncoimmunology. Cell 2016;164:1233-1247.
3) **El-Khoueiry AB**, **Sangro B**, Yau T, Crocenzi TS, Kudo M, Hsu C, et al. Nivolumab in patients with advanced hepatocellular carcinoma (CheckMate 040): an open-label, non-comparative,

phase 1/2 dose escalation and expansion trial. Lancet 2017;389: 2492-2502.
4) Chew V, Lai L, Pan L, Lim CJ, Li J, Ong R, et al. Delineation of an immunosuppressive gradient in hepatocellular carcinoma using high-dimensional proteomic and transcriptomic analyses. Proc Natl Acad Sci U S A 2017;114:E5900-E5909.
5) Sia D, Jiao Y, Martinez-Quetglas I, Kuchuk O, Villacorta-Martin C, Castro de Moura M, et al. Identification of an immune-specific class of hepatocellular carcinoma, based on molecular features. Gastroenterology 2017;153:812-826.
6) Kurebayashi Y, Emoto K, Hayashi Y, Kamiyama I, Ohtsuka T, Asamura H, Sakamoto M. Comprehensive immune profiling of lung adenocarcinomas reveals four immunosubtypes with plasma cell subtype a negative indicator. Cancer Immunol Res 2016;4: 234-247.
7) Tsujikawa T, Kumar S, Borkar RN, Azimi V, Thibault G, Chang YH, et al. Quantitative multiplex immunohistochemistry reveals myeloid-inflamed tumor-immune complexity associated with poor prognosis. Cell Rep 2017;19:203-217.
8) Angelo M, Bendall SC, Finck R, Hale MB, Hitzman C, Borowsky AD, et al. Multiplexed ion beam imaging of human breast tumors. Nat Med 2014;20:436-442.
9) Lozano R, Naghavi M, Foreman K, Lim S, Shibuya K, Aboyans V, et al. Global and regional mortality from 235 causes of death for 20 age groups in 1990 and 2010: a systematic analysis for the Global Burden of Disease Study 2010. Lancet 2012;380:2095-2128.
10) Pang YL, Zhang HG, Peng JR, Pang XW, Yu S, Xing Q, et al. The immunosuppressive tumor microenvironment in hepatocellular carcinoma. Cancer Immunol Immunother 2009;58:877-886.
11) Chew V, Chen J, Lee D, Loh E, Lee J, Lim KH, et al. Chemokine-driven lymphocyte infiltration: an early intratumoural event determining long-term survival in resectable hepatocellular carcinoma. Gut 2012;61:427-438.
12) Wada Y, Nakashima O, Kutami R, Yamamoto O, Kojiro M. Clinicopathological study on hepatocellular carcinoma with lymphocytic infiltration. HEPATOLOGY 1998;27:407-414.
13) Unitt E, Rushbrook SM, Marshall A, Davies S, Gibbs P, Morris LS, et al. Compromised lymphocytes infiltrate hepatocellular carcinoma: the role of T-regulatory cells. HEPATOLOGY 2005;41: 722-730.
14) Mathai AM, Kapadia MJ, Alexander J, Kernochan LE, Swanson PE, Yeh MM. Role of Foxp3-positive tumor-infiltrating lymphocytes in the histologic features and clinical outcomes of hepatocellular carcinoma. Am J Surg Pathol 2012;36:980-986.
15) Liu RX, Wei Y, Zeng QH, Chan KW, Xiao X, Zhao XY, et al. Chemokine (C-X-C motif) receptor 3-positive B cells link interleukin-17 inflammation to protumorigenic macrophage polarization in human hepatocellular carcinoma. HEPATOLOGY 2015;62:1779-1790.
16) Garnelo M, Tan A, Her Z, Yeong J, Lim CJ, Chen J, et al. Interaction between tumour-infiltrating B cells and T cells controls the progression of hepatocellular carcinoma. Gut 2017;66: 342-351.
17) Shi JY, Gao Q, Wang ZC, Zhou J, Wang XY, Min ZH, et al. Margin-infiltrating CD20(+) B cells display an atypical memory phenotype and correlate with favorable prognosis in hepatocellular carcinoma. Clin Cancer Res 2013;19:5994-6005.
18) Sakamoto M, Effendi K, Masugi Y. Molecular diagnosis of multistage hepatocarcinogenesis. Jpn J Clin Oncol 2010;40:891-896.
19) David FP, Rougemont J, Deplancke B. GETPrime 2.0: gene- and transcript-specific qPCR primers for 13 species including polymorphisms. Nucleic Acids Res 2017;45:D56-D60.
20) Saeed AI, Sharov V, White J, Li J, Liang W, Bhagabati N, et al. TM4: a free, open-source system for microarray data management and analysis. Biotechniques 2003;34:374-378.
21) Zucman-Rossi J, Villanueva A, Nault JC, Llovet JM. Genetic landscape and biomarkers of hepatocellular carcinoma. Gastroenterology 2015;149:1226-1239.e4.
22) Cancer Genome Atlas Research Network. Comprehensive and integrative genomic characterization of hepatocellular carcinoma. Cell 2017;169:1327-1341.e23.
23) Tsujikawa H, Masugi Y, Yamazaki K, Itano O, Kitagawa Y, Sakamoto M. Immunohistochemical molecular analysis indicates hepatocellular carcinoma subgroups that reflect tumor aggressiveness. Hum Pathol 2016;50:24-33.
24) **Tan PS**, **Nakagawa S**, **Goossens N**, Venkatesh A, Huang T, Ward SC, et al. Clinicopathological indices to predict hepatocellular carcinoma molecular classification. Liver Int 2016;36:108-118.
25) Hoshida Y, Nijman SM, Kobayashi M, Chan JA, Brunet JP, Chiang DY, et al. Integrative transcriptome analysis reveals common molecular subclasses of human hepatocellular carcinoma. Cancer Res 2009;69:7385-7392.
26) Boyault S, Rickman DS, de Reynies A, Balabaud C, Rebouissou S, Jeannot E, et al. Transcriptome classification of HCC is related to gene alterations and to new therapeutic targets. HEPATOLOGY 2007;45:42-52.
27) Labgaa I, Stueck A, Ward SC. Lymphoepithelioma-like carcinoma in liver. Am J Pathol 2017;187:1438-1444.
28) Salomao M, Remotti H, Vaughan R, Siegel AB, Lefkowitch JH, Moreira RK. The steatohepatitic variant of hepatocellular carcinoma and its association with underlying steatohepatitis. Hum Pathol 2012;43:737-746.
29) **Zhang JP**, **Yan J**, Xu J, Pang XH, Chen MS, Li L, et al. Increased intratumoral IL-17-producing cells correlate with poor survival in hepatocellular carcinoma patients. J Hepatol 2009;50: 980-989.
30) Peng D, Kryczek I, Nagarsheth N, Zhao L, Wei S, Wang W, et al. Epigenetic silencing of TH1-type chemokines shapes tumour immunity and immunotherapy. Nature 2015;527:249-253.
31) Xu W, Joo H, Clayton S, Dullaers M, Herve MC, Blankenship D, et al. Macrophages induce differentiation of plasma cells through CXCL10/IP-10. J Exp Med 2012;209:1813-1823, S1-S2.
32) Kong LQ, Zhu XD, Xu HX, Zhang JB, Lu L, Wang WQ, et al. The clinical significance of the $CD163^+$ and $CD68^+$ macrophages in patients with hepatocellular carcinoma. PLoS One 2013;8:e59771.
33) Li JQ, Yu XJ, Wang YC, Huang LY, Liu CQ, Zheng L, et al. Distinct patterns and prognostic values of tumor-infiltrating macrophages in hepatocellular carcinoma and gastric cancer. J Transl Med 2017;15:37.
34) **Zhang Y**, **Li JQ**, Jiang ZZ, Li L, Wu Y, Zheng L. CD169 identifies an anti-tumour macrophage subpopulation in human hepatocellular carcinoma. J Pathol 2016;239:231-241.
35) Calderaro J, Rousseau B, Amaddeo G, Mercey M, Charpy C, Costentin C, et al. Programmed death ligand 1 expression in hepatocellular carcinoma: relationship with clinical and pathological features. HEPATOLOGY 2016;64:2038-2046.
36) **Shen P**, **Roch T**, Lampropoulou V, O'Connor RA, Stervbo U, Hilgenberg E, et al. IL-35-producing B cells are critical regulators of immunity during autoimmune and infectious diseases. Nature 2014;507:366-370.
37) Matsumoto M, Baba A, Yokota T, Nishikawa H, Ohkawa Y, Kayama H, et al. Interleukin-10-producing plasmablasts exert

regulatory function in autoimmune inflammation. Immunity 2014;41:1040-1051.
38) **Andreu P**, **Johansson M**, **Affara NI**, Pucci F, Tan T, Junankar S, et al. FcRgamma activation regulates inflammation-associated squamous carcinogenesis. Cancer Cell 2010;17:121-134.
39) Fu YP, Yi Y, Cai XY, Sun J, Ni XC, He HW, et al. Overexpression of interleukin-35 associates with hepatocellular carcinoma aggressiveness and recurrence after curative resection. Br J Cancer 2016;114:767-776.
40) Budhu A, Forgues M, Ye QH, Jia HL, He P, Zanetti KA, et al. Prediction of venous metastases, recurrence, and prognosis in hepatocellular carcinoma based on a unique immune response signature of the liver microenvironment. Cancer Cell 2006;10: 99-111.
41) Calderaro J, Couchy G, Imbeaud S, Amaddeo G, Letouze E, Blanc JF, et al. Histological subtypes of hepatocellular carcinoma are related to gene mutations and molecular tumour classification. J Hepatol 2017;67:727-738.
42) Spranger S, Bao R, Gajewski TF. Melanoma-intrinsic beta-catenin signalling prevents anti-tumour immunity. Nature 2015; 523:231-235.

Author names in bold designate shared co–first authorship.

Supporting Information

Additional Supporting Information may be found at onlinelibrary.wiley.com/doi/10.1002/hep.29904/suppinfo.